Journal of
Ceramic Science
and Technology

J. Ceram. Sci. Tech., 07 [03] 243-248 (2016)
DOI: 10.4416/JCST2015-00083
available online at: http://www.ceramic-science.com

Microwave Dielectric Properties of (1-x)$CaTiO_3$-x($Na_{0.5}Nd_{0.5}$)TiO_3 Ceramics

A.E. Reda*, D.M. Ibrahim, D.A. Abdel Aziz

Ceramic Department, National Research Centre, 12622, Dokki, Cairo, Egypt.
received December 8, 2015; received in revised form February 20, 2016; accepted March 8, 2016

Abstract

The crystal structures, phase compositions and the microwave dielectric properties of (1-x)$Ca^{2+}TiO_3$ - x($Na^{1+}_{0.5}Nd^{3+}_{0.5}$)$TiO_3$ ceramics prepared by the conventional solid state route have been investigated. The formation of solid solution is confirmed in XRD patterns. A specimen using 0.92$Ca^{2+}TiO_3$-0.08($Na^{1+}_{0.5}Nd^{3+}_{0.5}$)$TiO_3$ (x = 0.08) sintered at 1250 °C/2 h possesses an excellent combination of microwave dielectric properties, (ε_r) = 31.8, a maximum (Qxf) value of $2 \cdot 10^4$ at 5 GHz. This may be related to the increase in density as well as the grain morphology, which led to a reduction in the dielectric loss to a value of $0.25 \cdot 10^{-3}$. It is proposed as a suitable candidate material for small-sized GPS patch antennas.

Keywords: Microwave, dielectric properties, calcium titanate, sodium neodymium titanate

I. Introduction

The growing importance of ceramic dielectrics for applications as microwave oscillators, filters, etc., has led to great advances in the material research and development of dielectric ceramic systems [1–3]. The materials used in microwave devices are required to have a high dielectric constant ε_r, high quality factor Q and a close-to-zero temperature coefficient of resonant frequency (TCF). In the early 1990s, ($RE_{0.5}Li_{0.5}$)TiO_3-$CaTiO_3$ (RE = rare-earth)-based solid solutions were first studied as potential resonator ceramics by Ezaki *et al.* [4]. Further work [5–8] focused on the Nd and Sm analogues. The $CaTiO_3$ (CT) system has ε_r = 160 and Qxf = 12 000 GHz while the $Li_{0.5}RE_{0.5}TiO_3$ (LRET) system typically has ε_r = 80 and Qxf = 6 000 GHz [6]. Each has a heavily distorted perovskite structure owing to rotations of the O octahedra and tuning through zero occurs because the LRET and CT have -ve and +ve values of τ_f, respectively. A wide range of MW properties has been reported for this system, which depends on the RE ionic radius and processing conditions [4–9].

Liang *et al.* [10] prepared (1-x)$Ca_{0.61}Nd_{0.26}TiO_3$-x$Nd(Zn_{0.5}Ti_{0.5})O_3$ (x = 0.00 – 0.40), referred to as (1-x)CNT-xNZT, by means of conventional solid-state preparation. Single orthorhombic perovskite phase was formed when x was less than 0.15. And a secondary phase Zn_2TiO_4 appeared for x = 0.20 while ZnO was the secondary phase for the ceramics with x above 0.20. The dielectric constant and temperature coefficient of resonant frequency decreased steadily with increasing x value. A high Qxf value above 10 000 GHz was achieved as x varied from 0.00 to 0.20. Some (1-x)CNT-xNZT ceramics with a high ε_r and high Qxf value were obtained: ε_r = 78.8, Qxf = 19 200 GHz, τ_f = +135 ppm/ K for x = 0.15; ε_r = 71.8, Qxf = 17 300 GHz, τ_f = +94 ppm/ K for x = 0.20.

Shen *et al.* [11] reported that a value for the dielectric constant (ε_r) equal to 24.61 and a Qxf value equal to 102 000 GHz were obtained for 0.85($Mg_{0.95}Ni_{0.05}$)TiO_3-0.15$Ca_{0.6}La_{0.8/3}TiO_3$ (85MNT-CLT) ceramic bodies sintered at 1325 °C for 4 h. They stated that this composition is suitable for application in microwave dielectric resonators and filters.

In this study, ($Na^{1+}_{0.5}Nd^{3+}_{0.5}$) TiO_3 was added to $Ca^{2+}TiO_3$ to make a ceramic system of (1-x) $Ca^{2+}TiO_3$ - x ($Na^{1+}_{0.5}Nd^{3+}_{0.5}$) TiO_3 with x = 0.08, 0.10, 0.20, 0.50 and 0.90. The resultant microwave dielectric properties were analyzed using densification, x-ray diffraction patterns and the microstructures of the ceramics. The correlation between the microstructure and the Q×f value was also investigated.

II. Experimental

Ceramic samples were prepared according to the solid-state route. Reagent grade $CaCO_3$ (98.5 – 100.5 %), Na_2CO_3 (≥ 99 %) (Sigma-Aldrich, Germany), TiO_2 (extra pure 99 – 100.5 %) (Riedel-de Haen, Sigma-Aldrich) and Nd_2O_3 (99 %) (S.D. Fine-Chem Ltd) powders as the starting materials were weighed according to the compositions (1-x) $Ca^{2+}TiO_3$ - x ($Na^{1+}_{0.5}Nd^{3+}_{0.5}$) TiO_3. The compositions with x = 0.08, 0.1, 0.2, 0.5 and 0.9 were denoted 92CT-NNT, 90CT-NNT, 80CT-NNT, 50CT-NNT, and 10CT-NNT, respectively. The starting materials were thoroughly mixed and ball-milled in appropriate stoichiometric ratios in distilled water for 24 h using agate balls in a planetary mill. The mixed/milled powders were then calcined at 1150 °C for 4 h. The calcined powders were then lightly ground by hand in a pestle and mortar and sieved through a 200-mesh screen. Secondary milling

* Corresponding author: aisha_ezz@yahoo.com

of the calcined powder was performed in distilled water for 24 h. These samples were mixed with polyvinyl alcohol (4 wt%) as a binder and uniaxially pressed into pellets of 10 mm diameter and 5 mm thickness on a hydraulic press (Seidner; Riedlinger type, Germany) under pressure of 20 MPa. To remove the binder, the samples were first heated up to 550 °C at a heating rate of 5 K/min with a soaking time of 2 h before being sintered in a temperature range of 1150 – 1300 °C with a heating rate of 10 K/min and soaking time of 2 h at each temperature. Structural analysis of samples using x-ray diffraction (XRD) analysis was performed between a 2θ range from 20° to 60° on a Philips Flex 2002 diffractometer using Cu Kα radiation (λ = 1.5418 Å), Ni-filter and a detector scan speed of 2°/min. Morphological investigations were performed on selected sintered bodies that had been polished and then thermally etched for 90 min at 150 °C below the sintering temperature. These were examined by means of scanning electron microscopy (SEM) and energy-dispersive x-ray (EDAX) using a JEOL JXA-840A Electron Probe Microanalyzer, Japan, equipped with an x-ray energy-dispersive spectrometer EDAX (INCA X-Sight, Oxford Instruments). The bulk density and apparent porosity of the sintered samples were measured with the conventional liquid displacement method. Microwave dielectric properties of the sintered samples were measured with a Vector Network Analyzer (VNA) in the frequency range from 50 MHz up to 13 GHz using the microwave resonator method [12].

III. Results and Discussion

(1) Mineralogical composition

(a) *X-ray diffraction analysis*

Fig. 1 indicates the single cubic perovskite phase of $CaTiO_3$-$Na_{0.5}Nd_{0.5}TiO_3$ with x = 0.08, 0.10, 0.20, 0.50 and 0.90 as the main constituent of (1-x)$CaTiO_3$-x($Na_{0.5}Nd_{0.5}$)TiO_3 ceramics sintered at 1250 °C/2 h. The x value increases up to 0.90 in the 10CT-NNT ceramic body that contains a high amount of $Na_{0.5}Nd_{0.5}TiO_3$ (x = 0.90), the $NdTiO_3$ phase appeared as secondary phase. It is understood that the crystal structure of $NdTiO_3$ is an orthorhombic phase. The formation of mixed phases in the CT-NNT ceramics system with high $Na_{0.5}Nd_{0.5}TiO_3$ content may be due to structural differences and because the average ionic radii of Na = 1.02 Å and Nd = 0.995 Å were larger than that of Ca = 0.99 Å. This result is in agreement with the results obtained by *Huang et al.* [13], who found that the formation of mixed phases in the 0.8($Mg_{0.95}Zn_{0.05}TiO_3$)-0.2$Ca_{0.61}Nd_{0.26}TiO_3$ ceramic system was due to structural differences and because the average ionic radius of the Ca^{2+} ion (0.99 nm) and Nd^{3+} (1.15 nm) were larger than that of Mg^{2+}(0.65 nm). Moreover, there was shift in the XRD peaks of the identified phase after sintering. The specimens of (1-x)$CaTiO_3$-x($Na_{0.5}Nd_{0.5}$)TiO_3 with the increasing ($Na_{0.5}Nd_{0.5}$)TiO_3 show a shift in the position of the XRD peaks to higher or lower diffraction angle directions as shown in Table 1. Reduced lattice parameters were obtained for higher substitution of neodymium (x = 0.20). A gradual shift of peak angles to the higher angle with slightly increasing percentage of neodymium percent reveals that the contraction of the perovskite lattice may be due to the smaller size of Nd^{3+} (0.995 Å) compared to the Na^{1+} ion (1.02 Å) [14]. However, the increase in lattice parameters in the specimen was based on Ti^{4+}site replacement by a larger cation than the Ti ion. So, $Na^{1+}$and Nd^{3+} ions could substitute the Ti^{4+} ion on the B-site, because the ionic radius of both Na^{1+} ion (1.02 Å) and Nd^{3+} (0.995 Å) were larger than Ti^{4+} ion (0.605 Å), which results in an increase in the unit cells [15].

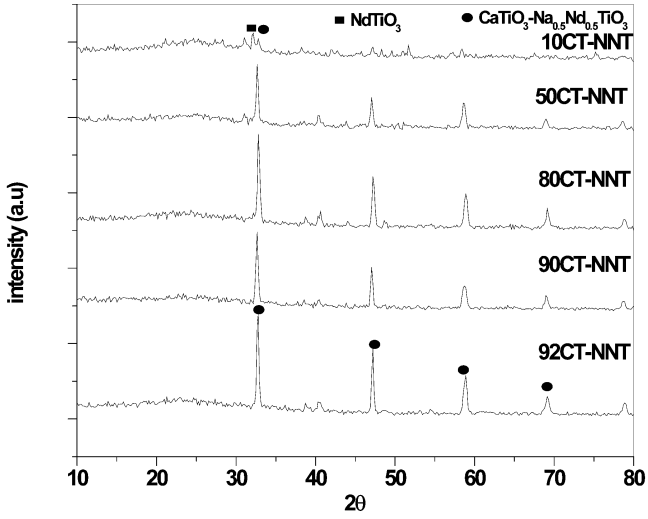

Fig. 1: XRD patterns of sintered (1-x)$CaTiO_3$-x($Na_{0.5}Nd_{0.5}$)TiO_3 ceramic bodies.

Table 1: Change in d-spacing (2θ) of peak with (1-x)$CaTiO_3$ -x($Na_{0.5}Nd_{0.5}$)TiO_3

Compositions	(2θ)
92CT-NNT	32.808
90CT-NNT	32.697
80CT-NNT	32.908
50CT-NNT	32.752
10CT-NNT	32.177

(b) *Microstructure of the sintered bodies*

SEM micrographs, Fig. 2(a-e), of (1-x)$CaTiO_3$-x($Na_{0.5}Nd_{0.5}$)TiO_3 ceramics with x = 0.08, 0.10, 0.20, 0.50 and 0.90 sintered at 1250 °C for 2 h show that the composition with lower ($Na_{0.5}Nd_{0.5}$)TiO_3 content appeared as a tree grain shape over the cubic perovskite structure with 92CT-NNT (x = 0.08) as seen in Fig. 2(a). Then, small spherical white particles appeared with (x = 0.10 and 0.20) with grain size (0.9 – 1.4 μm), which finally converted to cubic form (x = 0.50) with an increase in grain size up to 3.2 μm. Then, the grain size increase up to 6.7 μm with higher ($Na_{0.5}Nd_{0.5}$)TiO_3 content. The composition with x = 0.50 and 0.90 contains a high amount of small and large cubic-shape grains for $CaTiO_3$-$Na_{0.5}Nd_{0.5}TiO_3$ and platelet-like shapes that may be attributed to the presence of secondary phase.

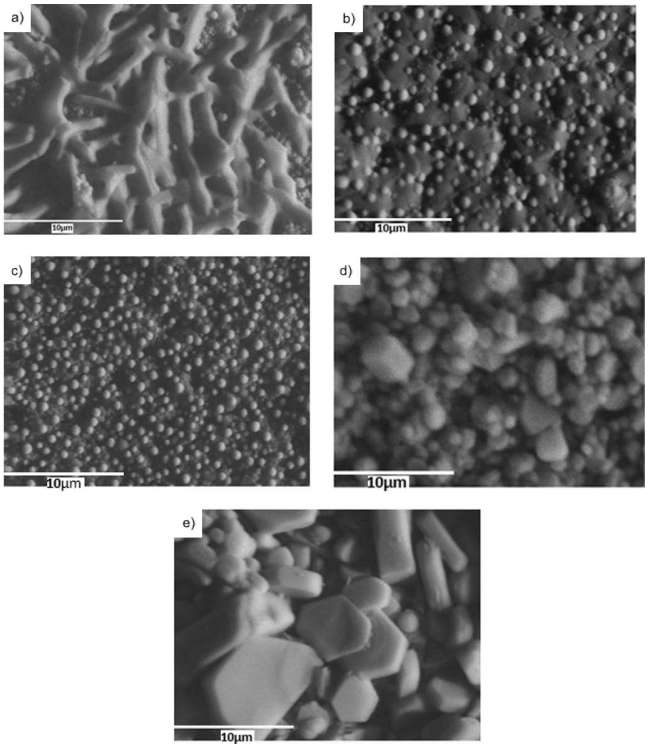

Fig. 2: Microstructure of (1-x)$CaTiO_3$-x($Na_{0.5}Nd_{0.5}$)TiO_3 at sintered temperature (a) x = 0.08 (92CT-NNT), (b) x = 0.10 (90CT-NNT), (c) x = 0.20 (80CT-NNT), (d) x = 0.50 (50CT-NNT) and (e) x = 0.90 (10CT-NNT).

(2) Densification parameters

The results for the bulk density of (1-x)$CaTiO_3$-x($Na_{0.5}Nd_{0.5}$)TiO_3 ceramics with various amounts of ($Na_{0.5}Nd_{0.5}$)TiO_3 with x = 0.08, 0.10, 0.20, 0.50 and 0.90 at different sintered temperatures from 1150 – 1300 °C for 2 h are shown in Fig. 3(a). The densities increased with increasing sintering temperature up to 1250 °C/2 h and ($Na_{0.5}Nd_{0.5}$)TiO_3 content up to x = 0.90 owing to the enlarged grain size up to 6.7 μm, as observed in Fig. 2(e). The increase in grain size resulted from the compacting of particles with each other during the sintering process, the transference happens from micro-sized to big particles because of the difference in the curvature radius. In this process, the coarsening of particle occurred, which resulted in a decrease in the surface energy [16]. The increase in bulk density with increasing sintering temperature may be due to the decrease in the number of pores, as observed in Fig. 3(b) and Table 2. A maximum density of 5.19 g/cm^3 was obtained for 10CT-NNT ceramic with x = 0.90. This implied that ($Na_{0.5}Nd_{0.5}$)TiO_3 can effectively increase the density with relatively low apparent porosity 0.58 % [2].

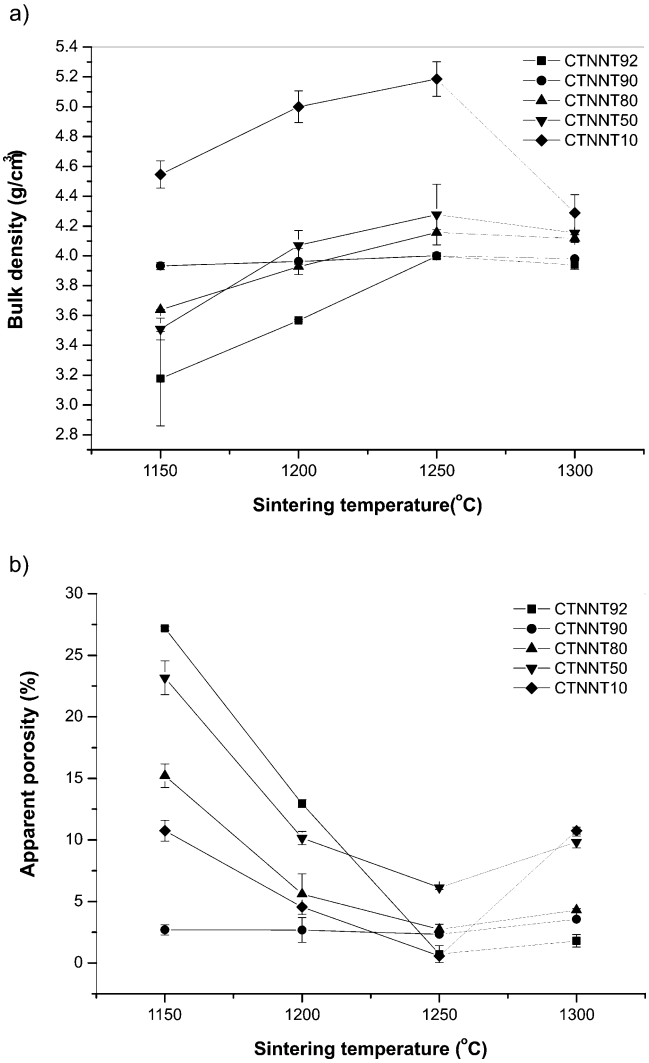

Fig. 3: Physical properties of (1-x)$CaTiO_3$-x($Na_{0.5}$ $Nd_{0.5}$)TiO_3 bodies at different sintered temperature.

Table 2: Physical and microwave dielectric properties of (1-x)$CaTiO_3$-x($Na_{0.5}Nd_{0.5}$)TiO_3 ceramic bodies at the same sintered temperature.

Samples	Bulk density, (g/cm^3) (1250°C)	Apparent porosity, (%)	Dielectric constant (ε_r)	Dielectric loss $\cdot 10^{-3}$	Quality factor (Q x f) $\cdot 10^4$ GHz
92CT-NNT	3.99 ± 0.0196	0.73 ± 0.686	31.8 ± 0.849	0.25 ± 0.007	1.99 ± 0.007 (5)
90CT-NNT	4.00 ± 0.0164	2.34 ± 0.128	27.1 ± 0.71	0.37 ± 0.007	1.4 ± 0.141 (5)
80CT-NNT	4.16 ± 0.0197	2.75 ± 0.416	21.2 ± 0.283	1.9 ± 0.07	0.32 ± 0.037 (6)
50CT-NNT	4.28 ± 0.203	6.15 ± 0.15	11.9 ± 0.141	2.5 ± 0.07	0.33 ± 0.0007 (8)
10CT-NNT	5.19 ± 0.116	0.58 ± 0.141	9.2 ± 0.283	4.2 ± 0.283	0.27 ± 0.014 (11)

(3) Microwave dielectric properties

Fig. 4(a) shows the variation of the dielectric constant (ε_r) measured at microwave frequency as a function of x = 0.08, 0.10, 0.20, 0.50 and 0.90 value for (1-x)$CaTiO_3$-x($Na_{0.5}Nd_{0.5}$)TiO_3 ceramics sintered at 1250 °C. The dielectric constant decreased slightly with increasing x($Na_{0.5}Nd_{0.5}$)TiO_3 content from (31.8 to 9.2). According to the Clausius-Mossotti equation, the dielectric constant increases with the increase in the total dielectric polarizability (αD) and the decrease in the unit cell volume. The effect of αD on the ε_r is greater than the role of the unit cell volume. A small change of αD results in a large variation with the increase in Na^{1+} (αD = 1.80 Å^3) compared with those of Nd^{3+} (5.01 Å^3), Ca^{2+} (3.16 Å^3) and Ti^{4+} (2.93 Å^3) [17–18]. Accordingly, the dielectric constant decreased with the sodium neodymium titanate content coinciding with that shown in Fig. 4(a).

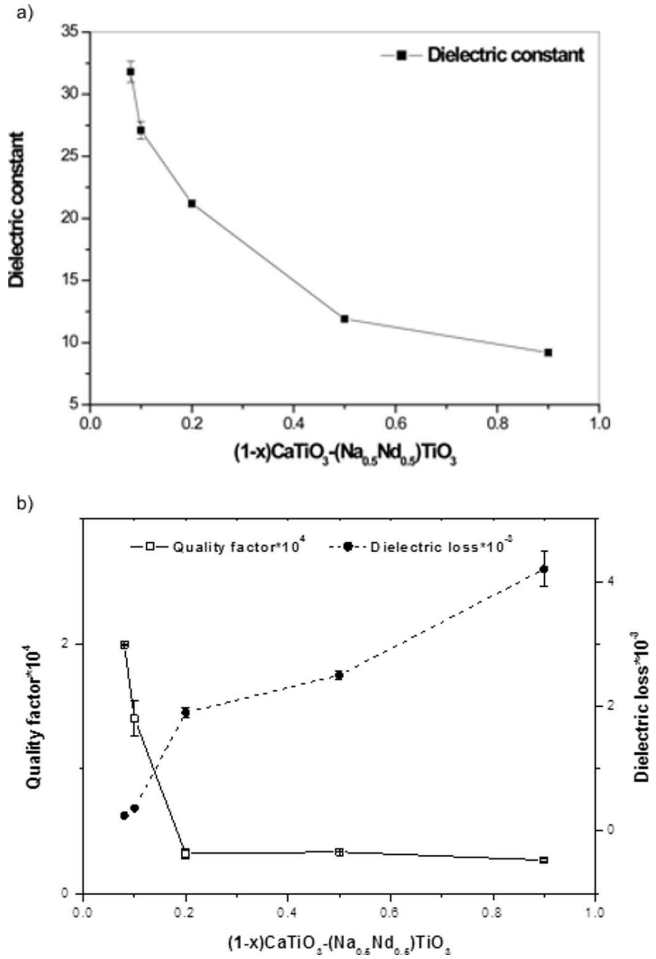

Fig. 4: Microwave dielectric properties of (1-x)$CaTiO_3$-x($Na_{0.5}Nd_{0.5}$) TiO_3 ceramics (a) dielectric constant (b) quality factor and dielectric loss as function of x value.

The calculated quality factors (Qxf) of (1-x)CT-x NNT ceramics with various x = 0.08, 0.10, 0.20, 0.50 and 0.90 content at sintered temperature is given in Fig. 4(b). The quality factor (Qxf) value decreased until a minimum value is allowed with x = 0.90, Table 2. It has been reported that the (Qxf) value is dependent on density, secondary phase and grain size. In this system, the effect of density could be neglected because the density reached a higher value with increasing x($Na_{0.5}Nd_{0.5}$)TiO_3 content, Table 2.

It is well known that many factors greatly affect the microwave dielectric loss and can be divided into two categories, intrinsic loss and extrinsic loss. Intrinsic losses are mainly caused by lattice vibration modes, while extrinsic losses are dominated by a second phase, oxygen vacancies, grain size, glassy phase and densification or porosity. So, a maximum Qxf value of $2{\cdot}10^4$ at 5 GHz for 92CT-NNT with x = 0.08 as compared with other samples. This may be related to grain morphology [19] as observed in Fig. 3(a), which led to a reduction in the dielectric loss value $0.25*10^{-3}$ as previously reported by Shen *et al.* [20].

A minimum (Qxf) value of $0.27*10^4$ at 11 GHz with high dielectric loss value $4.2*10^{-3}$, on the other hand, was attained for 10CT-NNT, Fig. 2(e). This may be attributed to the presence of secondary phase of $NdTiO_3$. Also, the microwave dielectric loss was caused not only by the lattice vibrational modes, but also by lattice defects and grain growth [13, 21].

IV. Conclusions

According to the results obtained in this study, it can be concluded that the addition of ($Na^{1+}_{0.5}Nd^{3+}_{0.5}$)$TiO_3$ to a $CaTiO_3$ composition plays an important role in the developed texture of the microstructure, densification and the microwave dielectric properties. The maximum result of sodium neodymium content was recorded for 92CT-NNT (x = 0.08) ceramic body sintered at 1250 °C/2 h, showing a (ε_r) = 31.8, maximum (Qxf) value of $2{\cdot}10^4$ at 5 GHz. This may be related to the increase in density as well as grain morphology, which led to a reduction in the dielectric loss to a value of $0.25{\cdot}10^{-3}$.

References

1 Wakino, K., Nishikawa, T., Ishikawa, Y., Tamura, H.: Dielectric resonator materials and their applications for mobile communication systems, *Brit. Ceram. Trans. J.*, **89**, [2], 39–43, (1990).

2 Sai, L., Lingxia, L., Xiaosong, L., Hao, S., Jing, Y.: Microwave dielectric properties of ZnO-doped $MgTiO_3$–($K_{0.5}La_{0.5}$)TiO_3 ceramic system, *Mater. Lett.*, **161**, 527–529, (2015).

3 Tianwen, Z., Ruzhong, Z., Chen, Z.: Preparation and microwave dielectric properties of $Li_3(Mg_{0.92}Zn_{0.08})_2NbO_6$-$Ba_3(VO_4)_2$ composite ceramics for LTCC applications, *Mater. Res. Bull.*, **68**, 109–114, (2015).

4 Ezaki, K., Baba, Y., Takahashi, H., Shibata, K., Nakano, S.: Microwave dielectric properties of CaO-Li_2O-Ln_2O ceramics, *Jpn. J. Appl. Phys.*, **32(9B)**, 4319–4322, (1993).

5 Takahashi, H., Baba, Y., Ezaki, K., Shibata, K.: Microwave dielectric properties and crystal structure of CaO-LiO-(1-x)Sm_2O_3-xLn_2O_3-TiO (Ln: lanthanide) ceramics system, *Jpn. J. Appl. Phys.*, **35(9B)**, 5069–5073, (1996).

6 Yoon, K.H., Chang, Y.H., Kim, W.S., Kim, J.B., Kim, E.S.: Dielectric properties of $Ca_{1-x}Sm_{2x/3}TiO_3$-li ceramics, *Jpn. J. Appl. Phys.*, **35(9B)**, 5145–5149, (1996).

7 Kim, J.S., Cheon, C., Kang, H.J., Lee, C.H., Yong, K., Nam, K.S., Byun, J.D.: Crystal structure and microwave dielectric properties of $CaTiO_3$-($Li_{1/2}Nd_{1/2}$)TiO_3-($Ln_{1/3}Nd_{1/3}$)TiO_3 (Ln=La, Dy) ceramics, *Jpn. J. Appl. Phys.*, **38(9B)**, 5633–5637, (1999).

8 Lowe, T., Azough, F., Freer, R.: The effect of $Bi_2Ti_2O_7$ addition upon the microwave dielectric properties of 0.4 $CaTiO_3$-$0.6Li_{0.5}Nd_{0.5}TiO_3$, *J. Eur. Ceram. Soc.*, **23**, 2429–2434, (2003).

9 Takahashi, H., Baba, Y., Ezaki, K., Okamoto, Y., Shibata, K., Kuroki, K., Nakano, S.: Dielectric characteristics of ceramics at microwave frequencies, *Jpn. J. Appl. Phys.*, **30**, 2339 – 2342, (1991).

10 Liang, B.L., Zheng, X.H., Tang, D.P.: New high-ε and high-Q microwave dielectric ceramics: (1-x)$Ca_{0.61}Nd_{0.26}TiO_3$-xNd($Zn_{0.5}Ti_{0.5}$)O_3, *J. Alloy. Compd.*, **488**, 409 – 413, (2009).

11 Shen, C.H., Huang, C.L., Shih, C.F., Huang, C.M.: A novel temperature-compensated microwave dielectric (1-x)($Mg_{0.95}Ni_{0.05}$)TiO_3 -x$Ca_{0.6}La_{0.8/3}TiO_3$ ceramics system, *Int. J. Appl. Ceram. Tec.*, **6**, [5], 562 – 570, (2009).

12 Wheless, W.P., Kajfez, D.: Experimental characterization of multimode microwave resonator using automated network analyzer, *IEEE T, Microw. Theory*, **MTT-35**, 12, 1263 – 1270, (1987).

13 Huang, C.L., Chen, Y.B., Tasi, C.F.: Influence of B_2O_3 additions to 0.8($Mg_{0.95}Zn_{0.05}$)TiO_3-0.2$Ca_{0.61}Nd_{0.26}TiO_3$ceramics on sintering behavior and microwave dielectric properties, *J. Alloy Compd.*, **460**, 675 – 679, (2008).

14 Dash, M.S.: Synthesis and electrical characterization of lanthanum doped barium titanate zirconate, National Institute of Technology, Rourkela-769008, India, 3 (2009).

15 Chen, Z., Xinyou, H., Hao, G., Chunhua, G.: Effect of Y_2O_3 & Dy_2O_3 on dielectric properties of $Ba_{0.7}Sr_{0.3}TiO_3$ series capacitor ceramics, *J. Rare Earth*, **25**, 197 – 200, (2007).

16 Reda, A.E., Ibrahim, D.M.M., Souya, E.R., Abdel Aziz, D.A.: Characterization and microwave dielectric properties of calcium titanate-sodium lanthanum titanate ceramics, *J. Appl. Sci. Res.*, **9**, [1], 541 – 547, (2013).

17 Shannon, R.D.: Dielectric polarizabilities of ions in oxides and fluorides, *J. Appl. Phys.*, **73**, [1], 348 – 366, (1993).

18 Fratello, V.J., Brandle, C.D.: Calculation of dielectric polarizabilities of perovskite substrate materials for high-temperature superconductors, *J. Mater. Res.*, **9**, [10], 2554 – 2560, (1994).

19 Hu, M., Luo, C., Tian, H., Gu, H.: Phase evolution, crystal structure and dielectric behavior of (1-x)Nd(Zn0.5Ti0.5)O_3 + xBi(Zn0.5Ti0.5)O_3 compound ceramics, **509**, 2993 – 2999, (2011).

20 Shen, C.H., Huang, C.L., Lin, L.M., Pan, C.L.: Characterization and dielectric behavior of B_2O_3-doped 0.9$Mg_{0.95}Co_{0.05}TiO_3$-0.1$Ca_{0.6}La_{0.8/3}TiO_3$ ceramic system at microwave frequency, *J. Alloy. Compd.*, **504**, 228 – 232, (2010).

21 Silverman, B.D.: Microwave absorption in cubic strontium titanate, *Phys. Rev.*, **125**, [6] 1921 – 1930, (1962).